UNIVERSITY OF LJUBLJANA

FACULTY OF PHARMACY

TIJANA MARKOVIČ

EVALUATION OF GLUCOCORTICOID INDUCED ATROPHY ON RECONSTRUCTED SKIN MODELS

OVREDNOTENJE Z GLUKOKORTIKOIDI POVZROČENE KOŽNE ATROFIJE NA TRIDIMENZIONALNIH KOŽNIH MODELIH

GRADUATION THESIS

Ljubljana, 2011

I performed this graduation thesis at the Institute for Pharmacy, Pharmacology and Toxicology, Free University of Berlin under the supervision of Prof. Dr. Monika Schäfer-Korting and with under the supervision of Assoc. Prof. Dr. Irena Mlinarič-Raščan, Faculty of Pharmacy, University of Ljubljana.

Acknowledgments

First, I would like to express my sincere gratitude to Prof. Dr. Monika Schäfer-Korting, Institute for Pharmacy, Pharmacology and Toxicology, Free University of Berlin, and to Assoc. Prof. Dr. Irena Mlinarič-Raščan, Faculty of pharmacy, University of Ljubljana, for giving me the opportunity to do my graduation thesis under their supervision and for their guidance and support. Next, I would like to thank Dr. Günther Weindl for being my working mentor, for his assistance, guidance, motivation, encouragement, positive working atmosphere and his assistance at writing of this thesis. I would like to thank my colleagues at the Institute for positive working environment. Then to my friends, who made my student years much more of the adventure than just sitting by the books. In the end, I would like to thank my parents and my sister for all the love and support.

Statement

I confirm this graduation thesis to be my own work done under supervision of Prof. Dr. Monika Schäfer-Korting and Assoc. Prof. Dr. Irena Mlinarič-Raščan.

Tijana Markovič

Abstract

Topical glucocorticoids (GCs) represent the most important treatment for epicutaneous therapy of inflammatory skin diseases. Besides the desired anti-inflammatory effects GCs also induce several adverse effects after prolonged GC therapy, among those, skin atrophy being the most frequently observed and due to its irreversibility a particularly serious condition. Thus, determining the atrophogenic potential of novel compounds is of importance for drug development.

The aim of the present study was to further develop an *in vitro* test system based on reconstructed skin models for the identification and characterization of GC-induced skin atrophy. The atrophogenic potential of topical GC-containing creams was evaluated on the reconstructed skin model EpidermFT and the results were compared to the Phenion model.

GC-class-specific reduction of IL-6 release in medium by GCs was obtained by ELISA in EpidermFT reconstructed skin equivalents for up to 14 days. Stronger GC-class specific reduction of IL-6 release was proven in PhenionFT model for period up to 7 days. Furthermore, as read out parameters predictive of atrophogenicity, the regulation of collagen and matrix metalloproteinase (MMP) gene expression, known to be suppressed by GC treatment, was analysed by Q-RT-PCR. A decrease of *COL1A1* mRNA expression was detected in the dermal compartment of EpidermFT models after 14 days of treatment with GC-containing creams and confirmed with immunofluorescence analysis of collagen type I. None of the collagens were found to undergo GC-regulation after 7 days GCs applications in EpidermFT nor in Phenion skin tissues. GCs were found to repress *MMP1* mRNA expression in the dermal compartment of EpidermFT models after 14 and 7 days of treatment. Moreover, *MMP1* mRNA levels were strongly reduced in the Phenion model after 7 days treatment. Thus, *COL1A1* and *MMP1* gene expressions were identified as reliable atrophy markers under the described experimental conditions.

Number of epidermal layers was severely reduced after 14 days and 7 days of treatment in EpidermFT and PhenionFT models with GC-containing creams and corresponding base cream formulations, thus the impact of GCs on epidermal thinning could not be evaluated. Noteworthy, cell nuclei were found in stratum corneum of cream- and TNF-treated samples.

In conclusion, the EpiDermFT (EFT-400-HCF) reconstructed skin model appears to be a useful test system to assess the anti-inflammatory and also atrophogenic effects of GCs.

Razširjeni povzetek

Glukokortikoidi predstavljajo najpomembnejšo terapijo pri vnetnih kožnih boleznih kot so kontaktni alergijski dermatitis (ekcem), luskavica in atopijski dermatitis. Poleg terapevtskih protivnetnih učinkov pa lahko daljša terapija s topičnimi glukokortikoidi povzroči tudi številne neželene učinke. Najpogostejše lokalne atrofične spremembe kože so tanjšanje kože, pojav strij in dilatacija površinskih žil. Med neželenimi učinki topičnih glukokortikoidov je najpomembnejša kožna atrofija, saj je najpogostejši neželeni učinek in je ireverzibilna. Razvoj novih glukokortikoidov in selektivnih agonistov glukokortikoidnih receptorjev z manj neželenimi učinki je cilj mnogih raziskovalnih projektov. Določanje atrofičnega potenciala novih steroidnih protivnetnih učinkovin predstavlja pomemben del pri razvoju novih učinkovin. Topikalni glukokortikoidi so v klasifikaciji po Nieder-ju razvrščeni v 4 razrede glede na njihovo jakost delovanja in neželene učinke: I) šibki do IV) zelo močni.

Glukokortikoidi se po difuziji v celico vežejo na receptorje za glukokortikoide, kar povzroči konformacijske spremembe, ki omogočijo translokacijo kompleksa iz citosola v jedro celice. V jedru reagira ligiran receptor za glukokortikoide z odzivnimi elementi za glukokortikoide ter pozitivno ali negativno modulira gensko ekspresijo. Glukokortikoidi inhibirajo gensko ekspresijo z vezavo ligiranih receptorjev za glukokortikoide na promotor vsebujoče negativne odzivne elemente za glukokortikoide ali z inhibicijo bazalnih transkripcijskih dejavnikov, kot sta AP-1 in NF-κB. NF-κB je heterodimer, ki večinoma tvori kompleks z inhibitorjem IκB. Glukokortiokoidi vplivajo na transkripcijsko aktivnost NF-κB preko povečanja IκB. Ta vezava prepreči translokacijo NF-κB v jedro in posledično transkripcije genov za vnetne proteine, kot so ciklooksigenaza, lipoksigenaza in provnetni citokini: tumor nekrozni faktor, interlevkin 1 in interlevkin 6. Glukokortikoidi preko protein-protein interakcij inhibirajo transkripcijo mnogih AP-1 in NF-κB reguliranih genov, kot so matriks metaloproteinaze.
Matriks metaloproteinaze (kolagenaze) so odgovorne za razgradnjo kolagena. Kolagenaza MMP1 ima sposobnost za hidrolitično cepitev trojne vijačnice kolagenov tipa I in III. Glukokortikoidi znižajo raven sinteze kolagena tip I in III ter nivo ekspresije informacijske RNA kolagenov. V koži so keratinociti v epidermisu in fibroblasti v dermisu glavne tarče delovanja glukokortikoidov.

Predvidljivi in evaluirani predklinični *in vitro* testni sistemi so potrebni za ovrednotenje tveganja za nastanek atrofije pri terapiji z novimi topičnimi glukokortikoidi. *In vitro* testni sistemi so v večini hitrejši, cenovno ugodnejši in zahtevajo manjše količine učinkovine v primerjavi z *in vivo* testnimi modeli, obenem so boljša izbira z vidika zaščite živali. Mednje sodijo monoplastne celične kulture humanih keratinocitov in fibroblastov.
Rezultat razvoja modernega tkivnega modeliranja so tridimenzionalni kožni modeli, ki predstavljajo povezavo med *in vivo* testnimi sistemi ter *in vitro* monoplastnimi celičnimi kulturami. Sestavljajo jih fibroblaste vsebujoča dermalna komponenta z ekstracelularnim matriksom, razvita bazalna membrana v dermalno/epidermalnem stiku ter stratificirana epidermalna komponenta. Epidermis je diferenciran v več plasti keratinocitov, kar omogoča možnost merjenja števila sloja keratinocitov. Dodatni prednosti tridimenzionalnih kožnih modelov pred monoplastnimi celičnimi kulturami sta možnost topikalnega nanosa glukokortikoidov v dermalnih formulacijah ter možnost ovrednotenja sinergističnega odziva keratinocitov in fibroblastov na terapijo z glukokortikoidi.

Namen te študije je bil nadaljevanje razvoja *in vitro* testnega sistema za identifikacijo in karakterizacijo z glukokortikoidi povzročene kožne atrofije na tridimenzionalnih kožnih modelih. S tem namenom so bile izvedene začetne študije na monoplastnih celičnih kulturah ter študije na tridimenzionalnem kožnem modelu EpidermFT. Izbrali smo dva glukokortikoida z različnima jakostima protivnetnega delovanja prednikarbat (razred II/III) in klobetazol propionat (razred IV) in različnima atrofičnima potencialnoma (prednikarbat < klobetazol propionat). Glukokortikoida smo v obliki krem Dermatop (prednikarbat 0,25%) in Dermoxin (klobetazol propionat 0,05%) nanašali vsak drug dan na tridimenzionalne kožne modele ter učinke po 14 dneh terapije primerjali s komplementarnima bazalnima kremama Dermatop in DAC ter kontrolo. Količina nanešene kreme 10 µl/cm^2 ustreza klinično nanešeni količini. Vnetne učinke smo preučevali z sistemsko aplikacijo tumor nekroznega farktorja v medij. Protivnetne učinke smo spremljali preko izločanja interlevkina 6 v medij z metodo encimskega imunskega testa. Za oceno stopnje atrofije smo ločili dermalni in epidermalni del tridimenzionalnega kožnega modela in v vsakem posebej preučevali nivo ekspresije informacijske RNA kolagenov in matriks metaloproteinaz z metodo Q-RT-PCR. Število slojev keratinocitov smo merili v 5µm histoloških sekcijah, barvanih s hematoksilinom in eozinom. Vpliv glukokortikoidov na kolagen smo določali z imunofluorescenco kolagena tipa I v histoloških sekcijah.

Preučevali smo vpliv glukokortikoidov v obliki topikalno nanešenih krem na protivnetno delovanje in nastanek atrofije na kožnem modelu EpidermFT v treh neodvisnih poskusih v paralelki. Protivnetno delovanje glukokortikoidov je bilo potrjeno z zaviranjem sproščanja interlevkina 6 v medij. Klobetazol propionat, glukokortikoid močnejše jakosti, je močneje zavrl sproščanje interlevkina 6 v medij kot prednikarbat v celotnem obdobju 14 dnevne terapije z glukokortikoidoma. Vnetno delovanje tumor nekroznega faktorja je bilo potrjeno z zvišanjem izločanja interlevkina 6 v medij.

Preučevanje optimizacije eksperimentalnih pogojev z menjavo medija vsak drug dan namesto vsakodnevno je pokazalo enake protivnetne učinke glukokortikoidov na zavrtje sproščanja interlevkina 6. Število slojev keratinocitov je bilo po 14 dneh inkubacije podobno znižano v obeh kontrolah, zaradi česar je smiselna optimizacija eksperimentalnih pogojev na menjavo medija vsak drug dan.

Vpliv topikalno nanešenih glukokortikoidov na nivo ekspresije informacijske RNA kolagenov in matriks metaloproteinaz, za katere je znano, da se po terapiji z glukokortikoidi znižajo, smo preučevali z metodo Q-RT-PCR. Glukokortikoida sta po 14 dneh znižala nivo ekspresije informacijske RNA *COL1A1* v dermalnem delu modela EpidermFT, znižanje kolagena tipa I je potrdila analiza z imunofluorescenco. Gen za kolagen tip I se ni znižal po 7 dneh terapije z glukokortikoidoma v EpidermFT in PhenionFT tkivnih ekvivalentih. Nivo ekspresije informacijske RNA *MMP1* se je znižal v dermalnem delu kožnega modela EpidermFT po 14 dneh ter po 7 dneh terapije z glukokortikoidi. V kožnem modelu PhenionFT je bil nivo ekspresije *MMP1* močno zavrt, kar je v povezavi z močnejšim zavrtjem nivoja interlevkina 6 v tem kožnem ekvivalentu. Ekspresija genov *COL1A1* ter *MMP1* je bila identificirana kot primerna za preučevanje z glukokortikoidi povzročene atrofije na tridimenzionalnem kožnem modelu EpiderFT po 14 dneh.

Evalvacija epidermalne debeline po terapiji z glukokortikoidi ni bila mogoča zaradi močno znižanega sloja keratinocitov po terapiji s kremama z glukokortikoidoma ter komplementarnima bazalnima kremama po 14 in 7 dneh v tridimenzionalnih kožnih modelih EpidermFT in PhenionFT.

V splošnem je naša študija potrdila tridimenzionalni kožni model EpidermFT kot primeren za ovrednotenje protivnetnega učinka glukokortikoidov in z glukokortikoidi povzročene kožne atrofije.

List of abbreviations and symbols

Abbreviations

ALDOA	fructse-biphosphate aldolase A
ALI	air liquid interface
AP-1	activating protein-1
bp	base pair
BSA	bovine serum albumin
cDNA	complementary DNA
COL(a)A1	collagen type (a), alpha 1
cP	clobetasol-17-propionate
ddH2O	double distilled water
DEX	dexametasone
DEPC	diethylpyrocarbonate
DMSO	dimethylsulfoxide
DNA	deoxyribonuclease
ECM	extracellular matrix
EDTA	ethylenediamin tetraacetic acid
ELISA	enzyme-linked immunosorbent assay
et al.	et alii (and others)
GAPDH	glyceraldehyde-3-phosphate dehydrogenase
GC	glucocorticoid
GCR	glucocoritcoid receptor
GRE	glucocorticoid response element
HAS	Hyaluronan synthase
H&E	hematoxylin & eosin
HMBS	porphobilinogen deaminase (hydroxymethylbilane synthase)
IκB	inhibitory κB
IL	interleukin
kB	kilo base
MMP	matrix metalloprotease
mRNA	messenger RNA
TMB	3,3',5,5'-Tetramethylbenzidine,
NF-κB	nuclear factor κB
P1NP	pro-collagen type I N terminal pro-peptide
PBS	phosphate-buffered saline
PC	prednicarbate
PCR	polymerase chain reaction
RNA	ribonucleic acid
RNase	ribonuclease
RPLP0	ribosomal protein large P0
RPL13A	ribosomal protein large 13A
RT	reverse transcription
SDHA	succine dehydrogenase flavoprotein subunit A
SEGRA	selective glucocorticoid receptor agonist
TBP	TATA-binding protein
TIMP	tissue inhibitor of metalloproteinase
TIX	therapeutic index

TNF	tumor necrosis factor
TRIS	Tris(hydroximethyl)aminomethan
YWHAZ	14-3-3- protein ζ/δ(protein kinase C inhibitror protein 1)

Symbols

µg	microgram
µm	micrometer
µM	micromolar
°C	celsius
h	hour(s)
M	mol/liter (concentration)
min	minute(s)
nM	nanomolar
rpm	rounds per minute
s	second(s)

Table of contents

1 INTRODUCTION

1.1 Structure of the human skin

The skin is the largest organ of the human body. One of its most important functions is a barrier to protect the body from external factors and to keep the internal systems intact. The skin is composed of the epidermis and of the dermis, two anatomically distinct layers connected by the basement membrane (Figure 1) (1, 2).

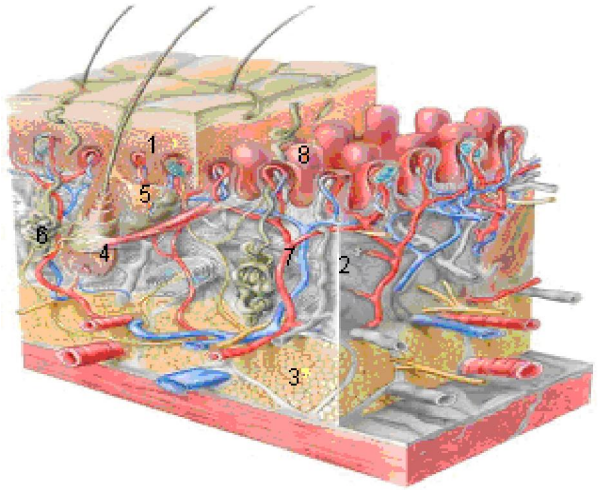

Figure 1: Structure of the skin and skin layers. 1 Epidermis, 2 Dermis, 3 Subcutis, 4 Hair follicle, 5 Sebaceous gland, 6 Sweat gland, 7 Blood vessel, 8 Papille (3).

Epidermis

Epidermis is an outer compartment of the skin and is about 100 µm thick. The main cells in epidermis are keratinocytes that present 90-95% of epidermal cells and produce the protein keratin. The four layers of epidermis represent the stages of maturation of keratin by keratinocytes. During the differentiation process, keratinocytes migrate from the basal proliferating cells into the upper layer of the epidermis. As keratinocytes die, they produce a cornified external membrane, the stratum corneum (horny layer). In the stratum corneum, the keratinocytes are embedded in a lipid-enriched extracellular matrix (ECM), which is responsible for the permeability barrier and provides mechanical resistance (Figure 2).

Maintenance of cell number in the epidermis depends upon a fine balance between proliferation and differentiation of keratinocytes. Interaction of keratinocytes with Langerhans cells, melanocytes, adhension to each other and basement membrane and interactions with underlying dermis are involved in the regulation of epidermal homeostasis (1, 2, 4).

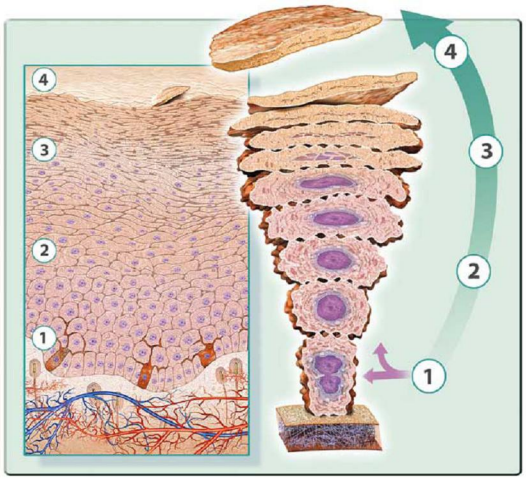

Figure 2: Schematic presentation of epidermis. Keratinocytes undergoing differentiation process from Stratum basale to Stratum corneum: 1 Stratum basale, 2 Stratum spinosum, 3 Stratum granulosum, 4 Stratum corneum (5).

Epidermis and dermis are connected through a basement membrane, which gives rise to epidermal cells. The basement membrane is a thin, though, flexible sheet of matrix. It contains specialized structures, called anchoring complex, which ensure stabile connections and allow communication between the two skin compartments (2, 6).

Dermis

Dermis is a connective tissue, consisting 70% of collagen fibres that impart strength and toughness to the skin. Elastin fibres are loosely arranged and give elasticity and firmness to the structure. The ground substance is a semi-solid matrix of glucosaminoglycans. Fibroblasts are the major cell type in dermis. They are responsible for production and degradation of collagens, elastin and glucosaminoglycans that form ECM. Type I collagen is the major skin collagen fibril, forming about 80 % of the skin collagen. The minor components are type III (10-15%) and V collagen (5 %). Collagens type IV, VII and XVII are found in the basement membrane. The dermis contains also sweat glands, hair follicles, nervous cells, nervous fibres and blood and lymph vessels. It provides nourishment for the epidermis, protection against injuries and water storage (1, 2, 6).

1.2 Inflammation and immunity of the skin

Besides the function of providing a physical barrier between internal organs and the environment, skin also actively functions as one of the principle outposts of the immune system. Insults to the skin are met by an integrated response by both resident cells and circulating migrant lymphoid cells in the skin that work in concert to produce cellular-derived soluble mediators – cytokines. When pro-inflammatory cytokines are released in the cutaneous environment, they can rapidly mobilize both the innate and cognate host immune system to limit or terminate the insulting agent. Other cutaneous cytokines have immunosuppressive, cell growth or proliferation activities.

The cytokines with pro-inflammatory activity such as tumour necrosis factor (TNF), interleukin (IL)-1 and IL-6 play a critical role in generating host responses against noxious agents, such as viral, fungal and bacterial pathogens as well as toxic chemicals, allergens and UV-light (8, 9).

In the skin, TNF can be produced by resident leukocytes, dendritic cells, keratinocytes, fibroblasts and mast cells. Biological activities of TNF are induction of proliferation of activated T and B cells, expression of certain major histocompatibility complex molecules and up-regulation of intercellular and vascular cell adhesion molecules (ICAM-1 and VCAM-1). The cytokine can act as angiogenesis factor and fibroblast growth factor and thus plays an important part in tissue remodelling after injury. The binding of TNF to its receptor actions in increased activity of specific target genes, such as nuclear factor (NF)-κB that controls the transcriptional regulation of a number of pro-inflammatory molecules (10). In addition, TNF stimulates the secretion of other pro-inflammatory cytokines, such as IL-1 and IL-6 and thus amplify its biological effects during local and systemic immune responses.

IL-6, like TNF and IL-1 is a pro-inflammatory cytokine. In the skin, it is produced by resident leukocytes, dendritic cells, keratinocytes, fibroblasts and endothelial cells. IL-6 principle activities are regulation of immunological responses, haematopoiesis and acute-phase reactions. This cytokine serves as a growth factor for activated B cells as well as a co-stimulator of T cell proliferation. IL-6 secretion can be induced by TNF and IL-1.

1.3 Glucocorticoids

Topical glucocorticoids (GCs) represent the most important treatment for epicutaneous therapy of inflammatory skin diseases such as eczema, psoriasis, erythema and irradiation diseases. With more than 50 years clinical experience, GCs are one of the best investigated drugs in clinical use. Besides the desired anti-inflammatory effects GCs also induce several adverse effects such as skin atrophy, steroidal acne and striae formation. Among those, skin atrophy is the most frequently observed and due to its irreversibility a particularly serious condition after topical long-term GC therapy (Figure 3) (11, 10, 12).

From a clinical point of view, skin atrophy can vary according to the potency of applied topical GC and in dependence on the pharmacokinetic conditions, respectively, as well as the duration of the application (13, 14). In addition, the vehicle in which the topical corticosteroid is formulated influences the absorption and thus potency of the drug (15).

Figure 3: GC-induced skin atrophy. Chronic topical GC use has led to thinning of the skin (29).

There is a wide variety of topical GC preparations containing various active ingredients and base preparations on the market, which can be ranked following their strength of effect (16). Topical GCs are classified according to their anti-inflammatory potencies after Niedner into four classes: I) weak, II) moderate, III) strong and IV) very strong (Table I). Thus, class I GCs like hydrocortisone have weak effects (regarding both desired anti-inflammatory effects and side effects) whereas class IV GCs like clobetasol 17-propionate (cP) have very strong effects (17). Moreover, it has been observed that GCs do not only show a different potency, but also a different benefit-to-risk ratio, which has been defined to improve the evaluation of the therapeutic benefit and the risk of adverse effects for a single topical GC from a clinical point of view (13, 14, 17).

Table I: Classification of GCs based on potency (modified after 18, 19).

Class	Effects	Examples
I	weak	Hydrocortisone, hydrocortisone acetate, prednisolone
II	moderate	Dexamethasone, prednicarbate
III	strong	Betamethasone 17-valerate, mometasone furoate
IV	very strong	Clobetasol 17-propionate

More recently, in addition to classification on potency, the therapeutic index (TIX) has been introduced for topical GCs (18). The TIX indicates the ratio of beneficial (potency in atopic dermatitis, vasoconstriction) and adverse (atrophogenicity, pituitary adrenal axis suppression and allergic potential) effects of several GCs and thus integrates its advantages and limitations. The concept of the benefit-to-risk ratio evaluation with topical GCs is based on both, *in vitro* and *in vivo* data, concerning efficacy and safety (20, 21, 22). Atrophy of the skin is the most prevalent side effect of topical administered GCs, therefore, the atrophogenic potential (Table II) is weighted more than other side effects for calculating the TIX (17).

Table II: Therapeutic indices and their potential to induce skin atrophy. Class: I = weak, IV = very strong. TIX = Therapeutic Index: 1≤2 relation between desired and adverse effect is equal, 2-3 means GC with improved benefit/risk ratio. Skin atrophy: 1 = GC induces little skin atrophy, 3 = GC induces much skin atrophy (Modified after 18, 19).

TIX	Skin atrophy	Class	Glucocorticoid
1	1	I	Hydrocortisone
1,2	2	III	Betamethasone 17-valerate
1,5	2	IV	Clobetasol 17-propionate
2	1	II	Prednicarbate
2	1	II	Methylprednisolone aceponate
2	1	III	Mometasone furoate

Atrophy, the most common adverse effect on the skin, appears as profound loss in skin thickness, shininess of the skin and the loss of elasticity (11). As a consequence, the skin surface becomes transparent, fragile and telangiectatic (23, 24, 25). The thinning of horny layer results in an increased permeability and transepidermal water loss, which indicates a disrupted barrier function of the skin (25, 27). Histopathologically, flat dermal-epidermal junctions (23), reduced thickness of epidermis (11), decreased size of keratinocytes (27), reduced number of fibroblasts (27), rearrangement of the geometry of the dermal fibrous network and a decrease of dermal collagen are found (28).

1.3.1 Molecular Mechanisms of GCs

Anti-inflammatory effects

GCs mediate their effects via many and diverse genomic and non-genomic mechanisms. After diffusion into the cell GCs interact with specific receptor proteins in the target cell, glucocorticoid receptors (GR). The ligand-mediated activation of the GR induces conformational changes that lead to translocation of the receptor from the cytosol into the nucleus. In the nucleus GR interacts with glucocorticoid-response elements (GRE) and modulates gene expression either positively (transactivation) or negatively (transrepression) (9, 16, 30) (Figure 4).

GR target genes that are positively regulated through the transactivation mechanism carry GC response elements (GRE) in the promoter or enhancer regions onto which GR can directly bind as homodimer (Figure 5 A). Via transcription of mRNA, an increased de novo synthesis of certain proteins takes place (31). The genes encoding proteins, which are directly induced by GCs, include lipocortin (annexin-1) and vasocortin. Lipocortin inhibits phospholipases (PLA) such as PLA-A2, which reduces the release of arachidonic acid and the synthesis of pro-inflammatory mediators such as prostaglandins, leukotrienes and platelet activating factor (32). Vasocortin inhibits histamine release and thereby exerts anti-allergic effects.

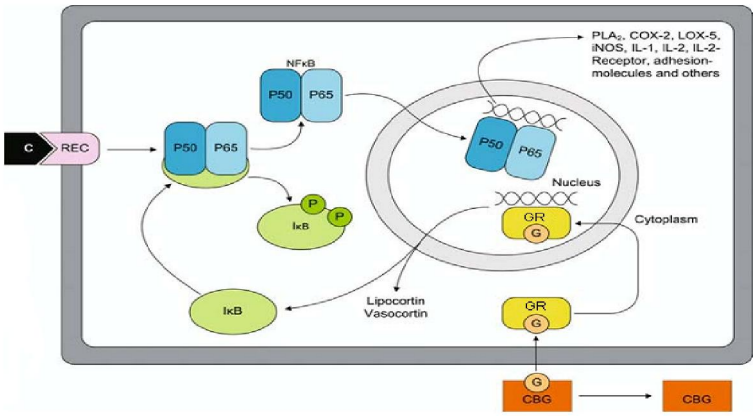

Figure 4: Molecular mechanisms of action of GCs. G glucocorticoids, REC receptor for C, C pro-inflammatory cytokines, CBG corticoid binding globulin, P50 and P60 subunits of NF-κB (32).

GCs inhibit gene expression either by binding of ligated monomers to a promoter containing negative GRE (nGRE) (Figure 5 B) or by inhibition of basal transcription factors such as AP-1 and NF-κB (10). NF-κB is a heterodimer, which generally forms a complex with its inhibitor IκB (Figure 4 and 5 G) (10, 33). This binding prevents translocation of NF-κB to the nucleus and subsequent transcription of genes encoding pro-inflammatory proteins such as cyclooxygenase (COX), lipoxygenase (LOX), PLA-A2, inducible nitric oxide (NO) synthetase, pro-inflammatory cytokines (TNF, IL-1, IL-6) and adhesion molecules (ICAM-1). GCs influence the transcriptional activity of NF-κB by increasing IκB, which binds and inactivates NF-κB (33). Another form of inhibited gene expression is by inhibitory protein–protein interactions of the GR with NF-κB and AP-1. This mechanism inhibits the transcription of various NF-κB- and AP-1-regulated genes such as IL-2 and collagenase (matrix metalloproteinase) (10, 32). In addition, ligated GR monomers form the complex with other essential transcription factors which then become inactivated (Figure 5 C-E) (10).

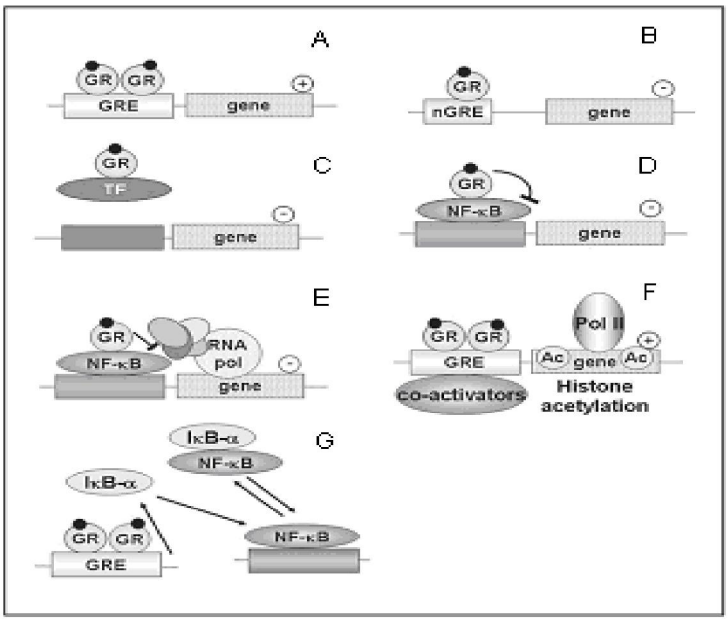

Figure 5: Models describing GC interactions with DNA and transcription factors
A Simple GRE, transactivation
B Binding of liganded monomers to a promoter containing negative GREs (nGREs)
C & E Sequestration or inhibition of basal transcription factors
D inactivation by masking of transactivation domains
F Increasing histone acetylation co-activators weaken histone-chromatine interactions which enables polymerase to initiate transcription, while the opposite holds true with histone deacetylase.
G Inhibition of the NF-κB pathway due to an enhanced transcription of the *IκBα* gene. (10, modified after 34).

Extracellular Matrix Protein Effects

In the skin, keratinocytes and fibroblasts are known target cells of GC action. An impaired synthesis and degradation of ECM proteins by GC treatment changes skin structure (7, 35). Alterations of the dermis mainly result from effects of GCs on collagen turnover (36, 37). Type I collagen is a heterodimer composed of two α1(I) chains and one α2(I) chain synthesized in a 2:1 ratio, which are encoded by *COL1A1* and *COL1A2* genes (38) and undergo post-translational modifications. GCs decrease the rates of type I collagen protein synthesis (39) and mRNA levels of *COL1A1* in fibroblasts (40). Collagen type III is synthesized as a homotrimeric procollagen comprising three identical α1(III) chains. GCs inhibitory effects on type III collagen at the protein level (41) as well as at the mRNA level (42) in fibroblasts have been found. Moreover, mRNA expression of *COL4A1*, *COL7A1*, *COL17A1* was found to be repressed by GC treatment (43).

Molecules participating in the collagen turn over, like matrix metalloproteinases (MMP), might also be affected by GCs (44, 45). The collagenase MMP-1 has the capacity to cleave the triple helix of type I and III collagen by hydrolysis (46). MMP-3 degrades in general denatured collagens (gelatines) and proteoglycans and activates MMP-1 (47). Besides final degradation of fibrillar collagens, MMP-2 and MMP-9 (gelatinase A and B) also degrade collagen type IV and remove unfolded or abnormal folded collagens (48). Activity of MMPs depends on interactions with ECM components and binding to endogenous inhibitors such as tissue inhibitor of metalloproteinases (TIMP) allowing a fast activation or deactivation of MMPs (49). Altered levels of MMPs can impair the structural integrity of the epidermis and the dermis and result in the remodelling of the skin. GC treatment of human skin was found to repress *MMP-1*, *MMP-2* and *MMP-9* mRNA expression (48, 49, 50). *MMP-1* and *MMP-3* mRNA expression is repressed by the activated GR via protein-protein interaction with AP-1 (49).

Dermal alterations caused by GCs are mainly due to an effect on the collagen turnover, however, regulation of other ECM proteins seems also to be involved in the development of atrophy (51). Indeed, decreases in production of hyaluronic acid (HA) and sulfated glycosaminoglycans have been described under treatment with GCs. Hyaluronic acid is produced by hyaluronan synthase (HAS) enzymes. In particularly, *HAS-2* mRNA expression was found to be repressed by GC treatment (52, 53, 54).

1.3.2 Cellular mechanisms of GCs

GC effects in epidermis

GC-induced atrophy in epidermis is likely to appear due to decreased size (55, 27) and suppressed proliferation of keratinocytes (57). Reasons for decreased cell size are not exactly known, but it is assumed that reduced biosynthesis of macromolecules of these cells might play an important role (58, 59). The anti-proliferative effect of GCs has been reported to be associated with reduced mitotic rates of GC-treated keratinocytes (60, 61). However, accelerated keratinocyte maturation results in thinning of the living epidermis due to the shorter epidermal cell life (55, 63, 64). It has been shown that topical GCs inhibit the terminal epidermal differentiation (65). The GC-induced epidermal thinning and especially the thinning of the stratum corneum are accompanied by an increased permeability and an increased transepidermal water loss (27), which generally indicates disrupted barrier function of the skin (26, 65).

GC effects in dermis

In dermal fibroblasts, GCs show antiproliferative effects (57, 66, 67) by reducing the mitotic rate of the cells (66). Hammer and co-workers demonstrated a protective activity of dexamethasone in primary human fibroblasts against TNF, UV- or ceramide-induced apoptosis (68). Thus, apoptosis appears not to be the reason for reduced numbers of fibroblasts. Fibroblasts play an important role in the synthesis of ECM proteins. GCs have been found to significantly interfere with the ECM protein production leading to thinning of the dermis.

1.4 Assessment of the atrophogenic potential of GCs

To determine the atrophogenic risk of newly developed compounds, predictive preclinical test systems are important. The currently preferred standard model for GC-induced skin atrophy in basic and pharmaceutical research is the model of hairless OFA hr/hr rats (69, 70). However, the limitation of many *in vivo* models is their limited predictivity for the situation in humans. The hairless rat seems to be more sensitive to GC-induced skin atrophy compared to humans. Moreover, *in vivo* models are labor-intensive, time- and compound-consuming and are not favorable experimental models with regard to aspects of animal protection. In contrast, *in vitro* test systems are in general fast, rather inexpensive and feasible with limited amounts of compounds. Thus, they are highly attractive, especially in early drug discovery and may also allow medium or even high throughput compound screening (9). Currently, only a few approaches have been described which allow, at least to some extent, the estimation of GC atrophogenic potential *in vitro*. They include assessment of basic experimental data regarding proliferation, collagen synthesis and molecular parameters using monolayer cultures. Nevertheless, the impact of topical formulations cannot be determined. In addition, crosstalk between different cell species and particularly between differently differentiated cells of one cell species is very limited. Therefore, reconstructed skin models represent a link between *in vitro* monolayer cell cultures and *in vivo* systems. Thus, the generation of mechanically stable three-dimensional skin equivalents marks a new era for the pharmacological characterization of newly developed compounds. Furthermore, this technology is pivotal for the characterization of raw materials used in cosmetics as the OECD guidelines do not permit the use of animal models since 2009, directive 2003/15/EC (71, 72). Reconstructed skin models are currently being tested for their use as a substitutes for animal models. Only one reconstructed skin model named PhenionFT (Henkel, Düsseldorf, Germany) was reported to be suitable to investigate skin atrophy parameters (9) (73). Moreover, our research group investigated another model EpidermFT by MatTek for GC-induced anti-inflammatory and atrophogenic effects (74). Thus, reconstructed skin models appear to be a promising alternative to *in vivo* studies for the characterization of novel compounds in drug research and development. Nevertheless, the development of compounds with anti-inflammatory effects such as GCs but with less side effects is within the focus of numerous programs within the pharmaceutical industry (73).

1.4.1 Reconstructed skin models

Modern tissue culture technology has made it possible to generate human skin equivalents that represent either reconstructed human epidermis (RHE) or epidermis and dermis connected in a reconstructed skin model *in vitro*. RHE became commercially available before reconstructed skin models, such as SkinEthic® (SkinEthic Nice, France) and EpiDerm™ (MatTek, Ashland, MA, USA). Reconstructed skin models found on the market include AST-2000 (CellSystems, St. Katharinen, Germany), PhenionFT® (Henkel, Düsseldorf, Germany) and EpiDermFT™ (MatTek) (Figure 6) among others. Commercially available skin equivalents and in-house models are used for safety analysis of cosmetics and toxicity screening of various pharmaceutical compounds (75).

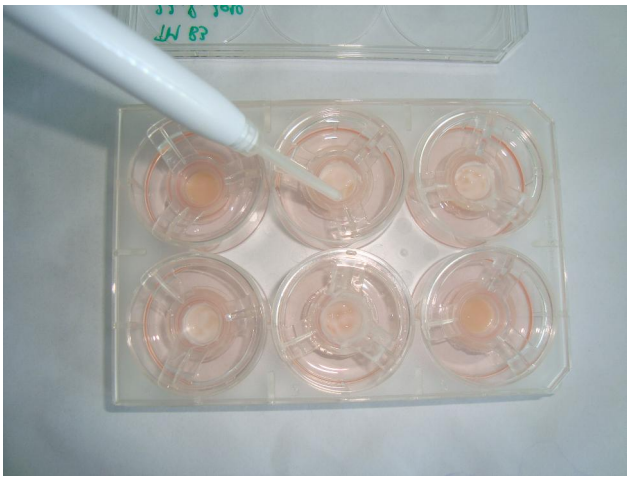

Figure 6: Reconstructed skin models EpiDermFT. MatTek EpidermFT skin equivalents are inserted into Costar Snapwell™ single well tissue culture plate.

Most protocols of skin models consist of a fibroblast-containing dermal component rich in ECM (75), a stratified epidermal component (76) and fully developed basement membrane at the dermal/epidermal junction (77). Typically, the skin equivalents consist of fibroblasts and keratinocytes derived from the same donor and isolated from human neonatal foreskin tissues. Normal human dermal fibroblasts are first seeded in a collagen I gel followed by seeding normal human epidermal keratinocytes on top. Differentiation of epidermis is induced by transferring the models to air/liquid interface (ALI) medium to produce stratified full-thickness skin equivalents (78). MatTek skin models are inserted into Costar

Snapwell™ single well tissue culture plates. In contrast, Phenion skin models are placed on a filter paper on special metal supports in cell culture dishes.

In three-dimensional skin models, keratinocytes are arranged in multilayer cell structures and hereby, epidermal thickness and dermal thinning can be determined in histological sections as a skin atrophy parameter. Immediately after a delivery, full differentiation of epidermis from stratum basale to stratum corneum can be observed in EpidermFT skin model (Figure 7) (79).

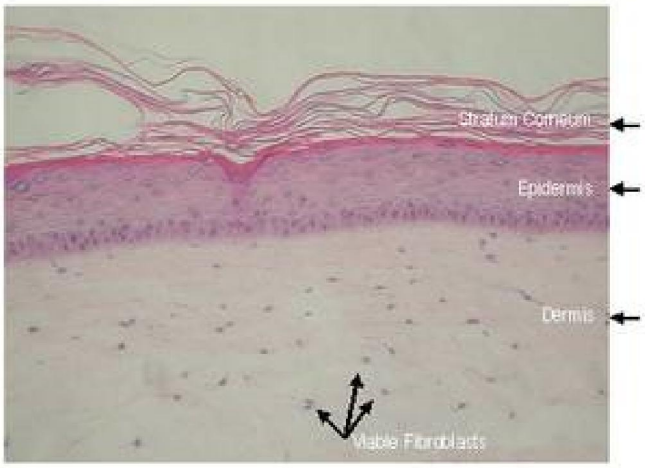

Figure 7: Histology of EpiDermFT. H&E Stained paraffin section reveals epidermis containing basal, spinous, granular keratinocytes and stratum corneum. Dermis contains numerous viable fibroblasts (79).

Recently, tissue culture technology has also been used to develop *in vitro* models of skin disease. The spectrum of model diseases available covers a range from inflammatory disease to cancer (75). A full-fledged model of allergic contact dermatitis is not available on the market, which is easy to understand considering the complexity required (75). One atopic dermatitis model described consists of immortalized keratinocytes (HaCaT cells) and human fibroblasts with added activated memory/effector T cells (81). There is an approach to produce allergic contact dermatitis reconstructed skin models based on Langerhans cells integrated into the suprabasal layers of RHE (75) and full-thickness skin constructs (80).

2 THE OVERALL AIM OF THE STUDY

The aim of this study will be to further develop an *in vitro* test system based on reconstructed skin models for the identification and characterization of GC-induced skin atrophy. Initial studies will be conducted on keratinocyte and fibroblast monolayer cell cultures to evaluate potential new atrophogenic markers (collagen VII, collagen XVII and hyaluronan synthase 2). Previously, the skin construct PhenionFT was reported to be suitable to investigate skin atrophy parameters. However, our research group showed that topical application of GC solutions for 7 days on EpiDermFT models revealed anti-inflammatory effects but not signs of GC-induced skin atrophy, known to appear only after prolonged treatment. Consequently, in the present diploma thesis experimental conditions of the EpiDermFT model will be modified to increase the potency of the test system in evaluating the atrophogenic potential of GCs. Two GC-containing creams, Dermatop (PC, 0,25%) and Dermoxin (cP 0,05%) with diverse anti-inflammatory potencies (cP class IV > cP class II/III) and different potential to induce skin atrophy (cP > PC) will be selected. The anti-inflammatory effects will be assessed by the release of IL-6 in the cell-free culture medium by ELISA. The GCs-induced reduction of cytokines release in the media will be evaluated to proof the GC anti-inflammatory effects. Inflammatory conditions in reconstructed skin models will be studied by systemic application of TNF. As read out parameters predictive of atropogenicity, the regulation of collagen and MMP gene expression will be analysed by Q-RT-PCR. Epidermal and dermal compartement will be separated for specific gene expression evaluation. Markers investigated will be *COL1A1, COL3A1, COL4A1, COL7A1, COL17A1, MMP1, MMP2* and *MMP9* mRNA expression upon topical GC-containing cream treatment. Downregulation of collagen and *MMP* mRNA expression levels will be evaluated to proof the atrophogenic potential of GCs treatment. Moreover, immunofluorescence of collagen type I will be assessed in histological sections. In addition to that, epidermal thickness will be determined in H&E stained histological sections as a major overall read out parameter of skin atrophy. In a last approach, comparative studies with topical application of two different GC-containing creams on EpiDermFT and PhenionFT models are going to be conducted.

3 MATERIALS AND METHODS

3.1 Materials

3.1.1 Laboratory apparatus, equipment, programs and machines

Table III: List of laboratory apparatus, equipment, programs and machines

Laboratory apparatus, equipment, program or machine	Manufacturer
Agagel Standard	Biometra, Göttingen, Germany
Autoclave, Tuttaner-System Sterilizer 2540ELV	Guwina-Hofmann, Berlin, Germany
Biowave DNA, WPA spectrophotometer	Biochrom, Cambridge, England
Blades 819, low profile	Leica Microsystems, Wetzlar, Germany
Disposable embedding molds (22 x 22 x 20 mm)	Polysciences, Warnington, PA, USA
Centrifuge Eppendorf 5415D	Eppendorf, Hamburg, Germany
Centrifuge Megafuge 1.0R	Heraeus, Hamburg, Germany
Centrifuge Tubes (15 ml and 50 ml)	Sarstedt, Nümbrecht, Germany
Clio Tube™ Vials	Nunc, Wiesbaden, Germany
Digital microscope, BZ-8000	Keyence, Nue-Isenburg, Germany
Easypet®	Eppendorf, Hamburg, Germany
Electrophoresis Chamber, Multigel long	Biometra, Göttingen, Germany
Filtration system Millipore®	Millipore, Schwalbach, Germany
Filtropur S 0.2 µm	Sarstedt, Nümbrecht, Germany
FLUOstar Optima	BMG Labtech,. Offenburg, Germany
Frigocut 2800 N	Leica, Bensheim, Germany
GraphPad Prism Software version 5	GraphPad software, San Diago, CA, USA
Hitachi 94 Chemistry Analyzer	Roche Diagnostics, Mannheim, Germany
Incubator BB 6220	Heraeus, Hanau, Germany
Lamin Air-Sterile Working Bench HB2472	Heraeus, Hanau, Germany
LightCycler® 480 Instrument	Roche Diagnostics, Mannheim, Germany
LightCycler® 480 Multiwell plate 96, clear	Roche Diagnostics, Mannheim, Germany
LightCycler® 480 Sealing Foil	Roche Diagnostics, Mannheim, Germany
LightCycler® 480 Software, Version 1.5	Roche Diagnostics, Mannheim, Germany
Magnetic Agitator IKAMAG® RCT	Janke & Kunkel, Staufen, Germany
Microman® M100 (10 - 100 µLµl)	Gilson, Middletown, WI, USA
Phase Contrast Inverted Microscope, Axiovert 135	Carl-Zeiss, Jena, Germany
Parafilm© M	Carl Roth, Karlsruhe, Germany
pH-Meter 766 Calimatec	Knick, Nürnberg, Germany
Pasteur pipettes	Carl Roth, Karlsruhe, Germany
Pippete Reference®	Eppendorf, Hamburg, Germany

Table III: List of laboratory apparatus, equipment, programs and machines

Laboratory apparatus, equipment, program or machine	Manufacturer
Pippete Research®	Eppendorf, Hamburg, Germany
Pippetes, TPP serological (5 ml, 10 ml and 25 ml)	TPP, Trasadingen, Switzerland
Pipetboy®	Integra Biosciences, Fernwald, Germany
Plates, Tissue culture (6-wells)	TPP, Trasadingen, Switzerland
Plates, ELISA (96-wells)	Greiner, Frickenhausen, Germany
Polyamide mesh 150 µm pore size	Neolab, Heidelberg, Germany
Safe-seal microtubes (0.5 ml, 1.5 ml and 2 ml)	Eppendorf, Hamburg, Germany
Scalpel, disposable	Feather, Osaka, Japan
Slides, microscope	Carl Roth, Karlsruhe, Germany
Stainless steal beads, 5 mm	Qiagen, Hilden, Germany
Standard Power Pack P25	Biometra, Göttingen, Germany
Surgical blades, sterile R (Nr. 11 and 24)	Greiner, Frickenhausen, Germany
Syringe (5 ml and 20 ml)	Carl Roth, Karlsruhe, Germany
Tips, pipette (10 µl, 100 µl and 1000 µl)	Sarstedt, Nümbrecht, Germany
Tips, Biosphere© (10 µl, 100 µl and 1000 µl)	Sarstedt, Nümbrecht, Germany
Tips, pipette Gilson (100 µl)	Gilson, Middletown, WI, USA
Tissue culture dishes (60 x 25mm)	TPP, Trasadingen, Switzerland
Tissue culture dishes (100 x 20mm)	TPP, Trasadingen, Switzerland
Tissuelyser II	Qiagen, Hilden, Germany
UV-Cuvettes micro (15 mm)	Brand, Wertheim, Germany
Vortexer	Heidolph, Kellheim, Germany
Water Bath DC3/W26	Haake, Karlshruhe, Germany

3.1.2 Chemicals

Table IV: List of chemicals

Chemical	Manufacturer
Acetic acid	VWR, Darmstadt, Germany
Agarose NEEO ultra quality	Carl Roth, Karlsruhe, Germany
Boric acid	Sigma-Aldrich, Steinheim, Germany
Calcium chloride ($CaCl_2$)	Carl Roth, Karlsruhe, Germany
Calcium chloride dihydrate ($CaCl_2 \cdot 2H_2O$)	Carl Roth, Karlsruhe, Germany
Diethylpyrocharbonate (DEPC)	Carl Roth, Karlsruhe, Germany
Citric acid, monohydrate	Carl Roth, Karlsruhe, Germany
Magnesium chloride ($MgCl_2$)	Carl Roth, Karlsruhe, Germany
Potassium chloride (KCl)	Carl Roth, Karlsruhe, Germany
Potassium di-hydrogen phosphate (KH_2PO_4)	Carl Roth, Karlsruhe, Germany
Potassium hydroxide (KOH)	Carl Roth, Karlsruhe, Germany
Sodium chloride (NaCl)	Carl Roth, Karlsruhe, Germany
di-Sodium hydrogen phosphate (Na_2HPO_4)	Carl Roth, Karlsruhe, Germany
Sodium dihydrogen phosphate (NaH_2PO_4)	Carl Roth, Karlsruhe, Germany

3.1.3 Solvents

Table V: List of solvents

Solvent	Manufacturer
Dimethyl sulfoxide (DMSO)	VWR, Darmstadt, Germany
Ethanol, 96%	Carl Roth, Karlsruhe, Germany
Ethanol, ≥99.8%	Carl Roth, Karlsruhe, Germany
Ethanol, absolute, extra pure	VWR, Darmstadt, Germany
Double distilled water (ddH_2O)	Institute of Pharmacy, Freie Universität Berlin, Berlin, Germany
Phosphate-buffered saline (PBS) w/o Ca^{2+}, Mg^{2+}	PAA Laboratories, Cölbe, Germany
Tris HCl (Trizma® HCl), 99%	Sigma-Aldrich, Steinheim, Germany
RNase-free H_2O	Sigma-Aldrich, Steinheim, Germany

3.1.4 Reagents

Table VI: List of reagents

Reagent	Manufacturer
3,3',5,5'-Tetramethylbenzidine	Carl Roth, Karlsruhe, Germany
Albumin, bovine fraction V powder	Carl Roth, Karlsruhe, Germany
ALI medium, HCT free	Phenion, Henkel AG & Co KgaA, Düsseldorf, Germany
Anti-collagen I, mouse IgG1	Dianova, Hamburg, Germany
Antifading Mounting Medium DAPI	Dianova, Hamburg, Germany
Bovine serum albumine BSA-c	Aurion, Wageningen, The Netherlands
DNase Amplification Grade I	Sigma-Aldrich, Steinheim, Germany
Dulbecco's Modified Eagle's Medium (DMEM)	Sigma-Aldrich, Steinheim, Germany
Eosin Y solutin 1% in water	Carl Roth, Karlsruhe, Germany
Ethylendiamin tetraacetic acid (EDTA)	Carl Roth, Karlsruhe, Germany
Fetal calf serum	Biochrom, Berlin, Germany
Formaldehyde, 4%	Carl Roth, Karlsruhe, Germany
GelRed™ Nucleic Acid Gel Stain, 10,000X In water	VWR, Darmstadt, Germany
GeneRuler™ 50 bp DNA ladder	Fermentas, ST. Leon-Rot, Germany
Goat Anti-Mouse IgG (H+L), DyLight 594	Dianova, Hamburg, Germany
Hematoxylin solution acid according to Ehrlich	Carl Roth, Karlsruhe, Germany
HEPES	Sigma-Aldrich, Steinheim, Germany
Hydrochloric acid (HCl)	Carl Roth, Karlsruhe, Germany
Hydrogen peroxide (H_2O_2), 30%	Carl Roth, Karlsruhe, Germany
IL-6 Duoset, human	R&D Systems, Wiesbaden, Germany

Table VI: List of reagents

Reagent	Manufacturer
LightCycler® 480 SYBR Green I Master	Roche Diagnostics, Mannheim, Germany
Medium EFT-400-HCF	MatTek Corporation, Ashland, MA, USA
Molecular biology grade water	Carl Roth, Karlsruhe, Germany
Nitrogen, liquid	Air Liquide, Berlin, Germany
Normal goat serum	Dianova, Hamburg, Germany
NucleoSpin® RNA II Kit	Macherey-Nagel, Düren, Germany
Primer	TIB Molibiol, Berlin, Germany
Proteinase K	Carl Roth, Karlsruhe, Germany
RevertAid™ First Strand cDNA Synthesis Kit	Fermentas, St. Leon-Rot, Germany
Roti® Histokit	Carl Roth, Karlsruhe, Germany
Sulfuric acid (H_2SO_4), 96%	VWR, Darmstadt, Germany
Thermolysin from *Bacillus thermoproteolyticus Rokko*, lyophilised	Sigma-Aldrich, Steinheim, Germany
Tumor necrosis factor (TNF), human recombinant	R&D Systems, Wiesbaden, Germany
Tween© 20	Carl Roth, Karlsruhe, Germany

3.1.5 Samples and substances

Table VII: List of biological samples and substances

Samples	Manufacturer
EpidermFT™ (EFT-412-HCF)	MatTek Corporation, Ashland, MA, USA
Phenion®-FT Skin model	Phenion, Henkel AG & Co KgaA, Düsseldorf, Germany
Substances	**Manufacturer**
DAC base cream	German Drug Codex (DAC)
Dematop® base cream	Sanofi-Aventis Deutschland GmbH, Frankfurt, Germany
Dermatop® cream 2.5mg/1g (prednicarbate)	Sanofi-Aventis Deutschland GmbH, Frankfurt, Germany
Dermoxin® cream 0.5 mg/1g (clobetasol17-propionate)	GlaxoSmithKline GmbH & Co., München, Germany

3.1.6 Culture media and solutions

Culture media and solutions used in this study were prepared as described.

Solutions for ELISA

Phosphate Buffered Saline (PBS), pH 7,2 – 7,4, in aqua bidestillata, autoclaved	
137 mM	NaCl
2.7 mM	KCl
8.1 mM	Na_2HPO_4
1.5 mM	KH_2PO_4

Wash buffer	
	PBS, pH 7.2 – 7.4, autoclaved
0.05%	Tween© 20

Reagent diluent, Block buffer	
	PBS, pH 7.2 – 7.4, autoclaved
1%	BSA

Substrate soultion (prepared fresh)	
	Citrate buffer
1%	TMB solution
0.3%	H_2O_2, 30%

Citrate buffer, 0,2 µm filtered	
40 mM	Citric acid, monohydrate
	ddH_2O
	adjusted to pH 3.95 with KOH

TMB solution, 0,2 µm filtered	
2%	3,3',5,5'-Tetramethylbenzidine
1:1	DMSO/Ethanol

Stop solution	
1N	HCl

Solution for separation of epidermis and dermis in reconstructed skin models

Thermolysin solution 0,5mg/ml	
33 mM	KCl
50 mM	NaCl
5 mM	$CaCl_2 \cdot 2H_2O$
0.01M	HEPES
0.5 mg/ml	Thermolysin from *Bacillus thermoproteolyticus Rokko*
	RNase-free H_2O

Solutions for agarose gel electrophoresis

10xTBE Buffer	
0.89 M	Tris base
20 Mm	EDTA
0.89 M	Boric acid
	ddH_2O

Solutions for quantification of RNA

Tris-HCl, pH 7,5	
10 mM	Tris base
	adjusted to pH 7.5 with HCl
	DEPC-treated H_20

Solutions for histology

4% formaldehyde in PBS, pH 7,4	
55 mM	Na_2HPO_4, anhydrous
12 mM	$NaH_2PO4 \cdot 2H_2O$
	ddH2O
4%	Formaldehyde, 36 – 40%

Solutions for immunofluorescence

Wash buffer and antibodies diluent	
	PBS, pH 7,2 – 7,4, autoclaved
0.0025%	BSA, 10%
0.025%	Tween 20

Blocking agent	
	PBS, pH 7.2 – 7.4, autoclaved
5%	Normal goat serum

3.2 Methods

3.2.1 Monolayer cell cultures

Keratinocytes and fibroblasts were maintained as previously published (74) and stimulated with the final concentrations 10^{-7} M (100 nM) and 10^{-9} M (1 nM) of prednicarbate (Pc) and clobetasol-17-propionate (Cp) in pure ethanol and DMSO, respectively. In chosen samples, an inflammatory response was included by adding TNF systemically to the medium at concentration 10ng/ml. After 72 hours treatment time, cells were lysed in RNA lysis buffer (see 3.2.2.3). Cell culture supernatants were transferred to 1.5-ml microcentrifuge tubes and centrifuged at 10,000g for 5 min at 4°C (74).

3.2.2 Reconstructed skin models

In the present study, two different commercially available human reconstructed skin models EpidermFT™, (MatTek) and PhenionFT model (Henkel) were used.

A multi-layered human full-thickness skin equivalents EpidermFT™ from MatTek consists of a fibroblast-containing dermal component rich in extracellular matrix (ECM), a stratified epidermal component and fully developed basement membrane at the dermal/epidermal junction. The skin equivalents consisted of fibroblasts and keratinocytes isolated from human neonatal foreskin tissue. Normal human dermal fibroblasts were seeded in a collagen I gel onto Costar Snapwell™ single well tissue culture plate inserts with a pore size of 0.4 μm, a diameter of 1.2 cm and surface area of 1.0 cm^2. Normal human epidermal keratinocytes were then seeded on top of the fibroblasts. The constructs were raised to the air/liquid interface and cultured for up to 21 days in serum-free culture medium to produce stratified, differentiation full-thickness skin equivalents. The skin models grew in hydrocortisone free media at least 3 days prior to shipment.

The PhenionFT model from Henkel is a multilayered equivalent of the human skin. The epidermis shows all natural skin structures from stratum basale to stratum corneum and is firmly joined to the underlying layer of fibroblasts which form the dermis. Normal human dermal fibroblasts were seeded in three-dimensional bovine collagene I scaffolds (1 cm^3) and cultivated for 14 days. Later, normal human epidermal keratinocytes were seeded on top of the scaffolds and the models were further propagated for 7 days. Differentiation of

epidermis was induced by transferring the models to ALI medium. The skin model has a diameter of 1.3 cm and surface area of 1.3 cm^2 and consists of keratinocytes and fibroblasts derived from the same human donor. The tissue pieces were handled according to the instructions of the manufacturer.

2.2.2.1 Treatment of reconstructed skin models with GCs creams, base creams and TNF

Immediately after arrival from USA on Tuesday afternoons after being shipped on Mondays, EpiDermFT™ tissues were incubated in 37°C with 5% CO^2 and saturated humidity. Tissues were incubated in 6-well microplates with pre-warmed 2 ml of hydrocortisone-free assay medium overnight.

Immediately after arrival from Düsseldorf, Germany on Tuesday afternoon, each specimen of Phenion model was transferred from the delivery plate on filter paper to the top of preplaced metal support into a 3.5 cm Petri dish. The latter was filled with approximately 5 ml of pre-warmed hydrocortisone free culture medium (37°C, Air Liquid Interface Medium, HCF). Six tissue pieces were then incubated for an equilibration period overnight at 37°C, with 5% CO_2 before examination.

To investigate long-term effects of treatment with GCs, MatTek and Phenion skin models were treated 14 and 7 days, respectively. The models were treated topically with GCs containing creams and base creams every other day. Additionally, to compare the effect of inflammatory conditions on the skin models itself, TNF was added systemically to one sample every other day.

Two commercially available GCs containing creams were used. Two comparable base creams were used and served as control. Dermatop® cream (2.5mg/1g) and Dermoxin® cream (0.5 mg/1g) contained weaker (class II) and strong (class IV) GCs, clobetasol 17-propionate (cP) and prednicarbate (Pc), respectively. Dermatop® (Cp 0.25%) and Dermatop® base cream were kindly provided by Sanofi-Aventis Deutschland GmbH (Frankfurt, Germany). DAC base cream was chosen to be the most appropriate alternative to Dermoxin base cream, which was not available for the present study. DAC base cream is being used on regular basis for dilution of GCs creams in community pharmacies in

Germany. Dermoxin® (Pc 0,05%) cream and DAC base cream were supplied from a local community pharmacy.

Using the topical regimen application, 10 µl/cm^2 cream was applied topically every second day with a positive displacement pipette (Microman, Gilson, Middletown, WI, USA). To improve spreading of creams, a nylon mesh (diameter 1.2 cm for MatTek and 1.3 cm for Phenion skin models) was placed on the surface of the all tissues prior the beginning of the experiments. This technique helped to keep the applied creams evenly distributed for the entire exposure period. The medium was replaced every other day by fresh and preheated medium, if not described differently. The skin models were exposed to GCs creams or base creams for 14 days, if not mentioned otherwise.

During the experiments, the media were collected for subsequent analysis of cytokine release by ELISA (see 3.2.2.2). At the end of the experiments, reconstructed skin models were washed twice with PBS and cut in halves (Figure 8), with exception of the first experiment. Halves of the models were prepared for histological and immunofluorescence analysis (see 3.2.2.4 and 3.2.2.5, respectively). For molecular analysis, epidermal and dermal compartment were separated with forceps and mRNA expression was analyzed (see 3.2.2.3).

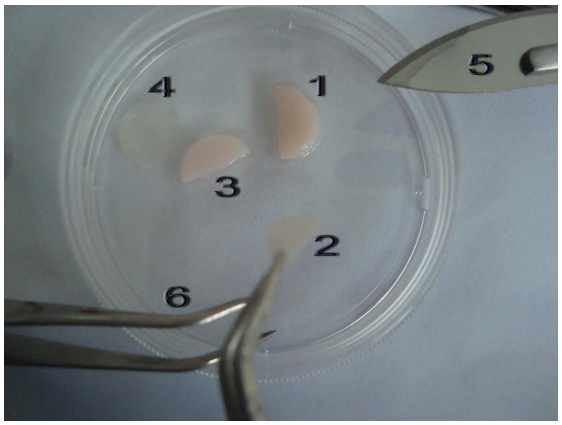

Figure 8: Reconstructed skin models EpidermFT after the treatment. The tissue equivalents were washed twice and processed for the further analysis.
1 half of the reconstructed skin model EpidermFT (histology and immunofluorescence)
2 epidermal compartment (mRNA expression) 3 dermal compartment (mRNA expression)
4 nylon mesh 5 surgical blade 6 forceps

Briefly, for each out of three batches of MatTek models, 12 skin models arrived. Experiments were performed as described previously in 6-wells in duplicates or simultaneously in two 6-wells with modified experimental conditions in one 6-well. For the first batch, 12 models were treated under described experimental conditions. At the end of experiment 6 models were prepared for further RT-PCR testing, whereas other 6 were processed for histological and immunofluorescence analysis. In the second batch, 6 models were treated as described, whereas the medium in other 6 skin equivalents was changed daily and TNF was applied daily, too. All 12 models from the second batch were cut in halves. Halves of the models were processed for further molecular biology analysis while other halves for cryosectional procedures. In the third batch, 6 MatTek skin equivalents were treated as previously described, whereas other 6 were treated the same way only for 7 days. At the end of third experiment, halves of skin models were prepared for further RT-PCR testing, whereas other halves were processed for histological and immunofluorescence analysis.

One batch of PhenionFT models was treated under described conditions for 7 days, simultaneously to the third batch of MatTek models. At the end of experiment, models were cut in halves. Halves of the models were processed for molecular biology testing. For this purpose, the epidermis and dermis were separated with Thermolysin from *Bacillus thermoproteolyticus Rokko* in HEPES buffer for 1 hour at 4ºC. The other halves were analyzed with histology and immunofluorescence.

3.2.2.2 Analysis of cytokine release by ELISA

Anti-inflammatory effects of GCs creams were assessed by sandwich ELISA. In order to determine the amount of released pro-inflammatory cytokines, the tissue medium was collected 48 hours after every treatment. Cell-free supernatants were assayed for IL-6 using commercial ELISA test kits (DuoSet, R&D Systems) according to manufacturers' instructions.

Briefly, 96-microwell plates were coated with 100 µl of IL-6 capture antibody overnight at room temperature. The next morning, capture antibody was three times washed with wash buffer and unspecific binding sites were blocked using block buffer. After one hour, 100 µl of cell-free supernatants diluted in reagent diluent were added in doubles. Simultaneously, standard solutions of recombinant human IL-6 diluted in reagent diluent to form seven-point standard curves using 2-fold dilutions and reagent diluent serving as a blank value were added in doubles. After two hours, unbound human cytokines were removed by three washes and 100 µl of detection antibody was added for two hours at room temperature. Aspiration and washes of the microwell plates were repeated three times. Next, streptavidin-horeseradish-peroxidase was bound to the complex for 20 minutes in the dark. After washing the plate, 100 µl of substrate solution was added forming the colorimetric reaction using tetramethylbenzidine (TMB) as a substrate for 20 minutes protected from light. Finally, 50 µl of stop solution was added. The absorbance of each well was determined immediately at the wavelength of 450 nm with a wavelength correction set at 570 nm in a scanning multiwall spectrophotometer (FluoStar Optima). The measured values of samples were computed according to the standard curve. The limit detection was 2.3 pg/ml of IL-6.

3.2.2.3 Measurement of mRNA expression

Isolation and quantification of total RNA

Total RNA from lysed monolayer cell cultures and homogenized epidermis and dermis from skin models was extracted using NucleoSpin® RNA II kit (Machinery-Nagel, Düren, Germany) according to manufacturer's protocol. In brief, halves of skin samples were frozen with liquid nitrogen and placed in 350 µl RNA lysis buffer and tissue lysate was denaturated with 3.5 µl of mercaptoethanol. Stainless steel beads were added and epidermis and dermis from MatTek and epidermis from Phenion models were homogenized using the Tissue Lyser II for 30 seconds at 25 Hz. Dermis from Phenion models was homogenized for 5 minutes. After homogenization, samples were centrifuged at 13,000 rpm for 30 seconds at 4ºC. Supernatants were transferred to fresh Eppendorf tubes and 300 µl RNase free water and 1.6 µl proteinase K was added. Next, samples were incubated at 55ºC for 10 minutes, allowing activation of proteinase K and again spun at 13000 rpm for 30 seconds at 4ºC. Samples were then processed using the RNA isolation protocol. Lysate was filtrated through NucleSpin filter to reduce viscosity and centrifuged for 1 minute at 11,000 g. RNA binding conditions were adjusted by adding 600 µl of 70% ethanol to the homogenized lysate, resulting in precipitation of nucleidic acids. DNA was bound by loading the precipitate to the NucleoSpin RNA II Column and centrifuged for 30 seconds at 11,000 g. The column was than placed into new collection tube and silica membrane was desalted by adding 350 µl membrane desalting buffer and centrifuging at 11,000 g for one minute to dry the membrane. DNA was digested by applying 95 µl DNase reaction mixture on the centre of silica membrane of the column and incubation at room temperature for 15 minutes. Next, silica membrane was washed twice by adding 200 µl and 600 µl of NucleoSpin II Buffer RA2 and RA3, respectively and span after each washing for 30 seconds. 250 µl of the latter was used one more time to wash silica membrane and centrifuged for 2 minutes to dry the membrane completely. Highly pure RNA was than eluted in 40 µl RNase free water and centrifuged at 11,000 g for 1 minute. Eluate was applied one more time to the column for re-elution and centrifuged at 11,000 g for 1 minute. Eluted RNA was immediately put on ice for optimal stability. Isolated RNA was stored at -80ºC until further analysis.

Isolated RNA was quantified using Biowave DNA, WPA spectrophotometer and micro UV-Cuvettes. 7 µl of isolated RNA was diluted with 63 µl of Tris-HCl buffer and absorbance at 260 nm and 280 nm was measured. The ratio between absorbance measured at 260 nm and 280 nm between 1.8 and 2.0 indicated highly pure RNA. Tris buffer was used as a blank value. Integrity of RNA was assessed with agarose gel electrophoresis, ensuring RNA did not degrade during isolation process.

DNase treatment and cDNA synthesis

Isolated and purified RNA was transcribed to complementary DNA (cDNA) using ReverdAid First Strand cDNA Synthesis Kit (Fermentas, ST. Leon-Rot, Germany) according to manufacturer´s protocol. Prior to cDNA synthesis, the RNA sampes were treated with DNase Amplification Grade according to manufacturer´s protocol (Sigma-Aldrich, Steinheim, Germany). Briefly, 1 µg of total RNA was incubated with 1 µl DNase and 1 µl reaction buffer in 10 µl reaction mixture for 10 minutes at 25ºC. DNase was inactivated by adding EDTA solution and incubation at 70ºC for 5 minutes. cDNA was synthesized by incubating DNase treated RNA, random hexamer primers, reaction buffer, dNTPs, RNase inhibitor and reverse transcriptase for 5 minutes at 25 ºC, followed by 1 hour at 42ºC. The reaction was inactivated by heating at 70ºC for 10 minutes and samples were chilled on ice. The synthesized cDNA was diluted 4-fold with nuclease-free water and stored at -20ºC until further analysis.

Q-RT-PCR

The polymerase chain reaction served to amplify the transcript cDNA previously obtained. Q-RT-PCR is a very sensitive and reliable method for gene expression analysis. All reactions were run on a LightCycler® 480 System. RT-PCR amplification mixture (10µl) contained template cDNA (1:5 dilution), 500 nM forward and reverse primer, and the LightCycler® 480 SYBR I Master. RT-PCRs were performed with a pre-denaturating step of 95°C for 5min and 45 cycles of 95°C (10 seconds), 60°C (10 seconds), and 72°C (10 seconds) followed by melting curve analysis and a final cooling step at 40°C for 10 seconds (see Table VIII).

Table VIII: PCR parameters of LightCycler® 480

Detection Format	**Block type**	**Reaction volume**
SYBR Green	96	10 µl
Programs		
Program name	**Cycles**	**Analysis mode**
Pre-incubation	1	None
Amplification	45	Quantification
Melting curve	1	Melting curves
Cooling	1	None
Temperature targets		

Target(°C)	**Aquisition Mode**	**Hold (hh:mm:ss)**	**Ramp rate (°C/s)**	**Aquisition (per °C)**
Pre-incubation				
95	None	00:05:00	4.4	/
Amplification				
95	None	00:00:10	4.4	/
60	None	00:00:10	2.2	/
72	Single	00:00:10	4.4	/
Melting curve				
95	None	00:00:05	4.4	/
65	None	00:01:00	2.2	/
97	Continuous	/	/	10
Cooling				
40	None	00:00:10	1.5	/

The crossing-point value from each signal was calculated based on the second derivative maximum method performed by LightCycler® 480 quantification software (version 1.5). PCR product sizes were checked on a 2% agarose gel. All corresponded to the expected size. Melting curves showed single amplified product for all genes and the melting curves were in accordance with those calculated. Specific primers were created using the Primer3 program (Table IX and X). To avoid nonspecific amplifications, primer sequences were blasted using Blast (NCBI). Primers were synthesized and dissolved in molecular grade water to a final concentration of 10 µM. A set of serially diluted cDNAs was used to construct a 6 data-point standard curve for every gene. The efficiency was more than 1.89 for all the primer pairs. Both standard and experimental samples were performed in duplicate and quantification of gene expression was achieved using the relative quantification method with efficiency correction.

Table IX: Primer sequences, expected product size and gene bank accession number for all reference genes analyzed.

Gene Gene bank No.	Sense Antisense	Primer sequence (5' → 3')	Base pairs
ALDOLASE NM_000034	Sense Antisense	CGGGAAGAAGGAGAACCTG GACCGCTCGGAGTGTACTTT	98
GAPDH NM_002046	Sense Antisense	CTCTCTGCTCCTCCTGTTCGAC TGAGCGATGTGGCTCGGCT	69
HMBS NM_000190	Sense Antisense	ACCAAGGAGCTTGAACATGC GAAAGACAACAGCATCATGAG	145
SDHA NM_004168	Sense Antisense	TGGGAACAAGAGGGCATCTG CCACCACTGCATCAAATTCAT	86
YWHAZ NM_000034	Sense Antisense	AGACGGAAGGTGCTGAGAAA GAAGCATTGGGGATCAAGAA	127
TBP NM_003194	Sense Antisense	TTCGGAGAGTTCTGGGATTGTA TGGACTGTTCTTCACTCTTGGC	227
RPLP0 NM_001002	Sense Antisense	GCTGCTGCCCGTGCTGGTG TGGTGCCCCTGGAGATTTTAGTGG	130
RPL13A NM_012423	Sense Antisense	CCTGGAGGAGAAGAGGAAAGAGA TTGAGGACCTCTGTGTATTTGTCAA	126

Table X: Primer sequences, expected product size and gene bank accession number for all target genes analyzed.

Gene Gene bank No.	Sense Antisense	Primer sequence (5' → 3')	Base pairs
COL1A1 NM_000088	Sense Antisense	CCTCAAGGGCTCCAACGA TCAATCACTGTCTTGCCCCA	117
COL3A1 NM_000090	Sense Antisense	GATCAGGCCAGTGGAAATGT GTGTGTTTCGTGCAACCATC	125
COL4A1 NM_001845	Sense Antisense	ACTCTTTTGTGATGCACACCA AAGCTGTAAGCGTTTGCGTA	151
COL7A1 NM_000094	Sense Antisense	GATGACCCACGGACAGAGTT ACTTCCCGTCTGTGATCAGG	118
COL17A1 NM_000494	Sense Antisense	TGTGCTGCAGCGGGATGACG CGGGGGACCAGGAAGCCCAA	187
IL-6 NM_000600	Sense Antisense	CACAGACAGCCACTCACCTC TTTTCTGCCAGTGCCTCTTT	137
MMP1 NM_002421	Sense Antisense	GGGAGATCATCGGGACAACTC GGGCCTGGTTGAAAAGCAT	72
MMP2 NM_004530	Sense Antisense	GCGGCGGTCACAGCTACTT CACGCTCTTCAGACTTTGGTTCT	71
MMP9 NM_004994	Sense Antisense	CCTGGAGACCTGAGAACCAATC CCACCCGAGTGTAACCATAGC	79
HAS2 NM_005326	Sense Antisense	CCTCATCATCCAAAGCCTGT GATGCAAAGGGCAACTGTTT	100

3.2.2.4 Histological analysis of reconstructed skin models

The epidermal thickness was assessed by histological analysis. Therefore, tissues were cut in halves and embedded in tissue freezing medium over liquid nitrogen steam. Sections with 5µm thickness were obtained using a cryotome. For analysis of epidermal thickness, frozen serial section were air dried for 10 minutes and stained with Mayer´s hematoxylin and eosin. Hematoxylin/eosin (H&E staining) is a widespread histological stain for a large number of different tissue structures. The major oxidization product of hematoxylin is hematin, which is responsible for the colour properties. It stains cell nuclei with good intracellular detail in blue, while eosin stains cytoplasm and connective tissue in a pink colour. In order to perform H&E stain, cryosections were fixed in 4% formaldehyde pH 7.4 for 5 minutes followed by immersion of the slides in double distilled water for 30 seconds. Slides were then treated for 5 minutes with hematoxylin and washed under running tap water for 5 minutes. Subsequently, slides were stained with eosin for 30 seconds. Dehydration of sections was performed with two charges of 96% ethanol for two minutes each, followed by two charges of 100% ethanol for two minutes each. Finally, ethanol was extracted with two charges of xylene for two minutes each and mounted with Roti®-Histokitt.

The number of epidermal cell layers (stratum basale to stratum granulosum) was visually determined using H&E stained sections with a digital microscope. For the determination of epidermal thickness, number of keratinocytes´ layers was counted from basal membrane to the upper limit of epidermis, underneath the stratum corneum. Epidermal thickness was determined at 5 different areas on 5 non-consecutive sections.

3.2.2.5 Immunofluorescence analysis of reconstructed skin models

The dermal thinning was assessed by immunofluorescence analysis of collagen I on skin models. Therefore, tissues were cut in halves and embedded in tissue freezing medium over liquid nitrogen steam. Sections with 5µm thickness were obtained using a cryotome. For analysis of dermal thinning, frozen serial section on objective glasses were air dried for 10 minutes. Next, cryosections were fixed in 4% formaldehyde pH 7.4 for 5 minutes followed by washing the slides first with PBS and next with PBS/BSA/Tween for 5 minutes each. Slides were then transferred to 5cm-Petri dishes and blocked with 2 ml of goat serum for 30 minutes at room temperature. After removal of goat serum, slides were coated with 400 µl of primary antibody (Anti-collagen I, mouse IgG1) for 60 minutes at room temperature. Washing with PBS/BSA/Tween was performed with three charges for ten minutes each. As secondary antibody, 400 µl of goat anti-mouse IgG (H+L), DyLight 594 conjugated was used per slide and incubated for 30 minutes in dark at room temperature. Again, slides were washed protected from light with 3 charges of PBS/BSA/Tween for ten minutes each. Finally, sections were mounted with one drop of antifading mounting Medium DAPI. Mounted slides were stored at 4ºC in the dark. The immunofluorescence was detected visually by determining dermal collagen in sections with a digital microscope. Collagen immunofluorescence was determined at 5 different areas on 5 non-consecutive sections. For quantification, unsaturated fluorescent images were thresholded, and pixel density was quantified using ImageJ (version 1.44, National Institutes of Health).

3.2.2.6 Statistics

Data are given as arithmetic mean ± standard error mean (SEM) and were calculated from three independent experiments, which were performed each in duplicate if not mentioned otherwise. Microsoft Excel version 2007 and GraphPad Prism Software version 5 (GraphPad software, San Diego, CA, USA) were used for analysis and presentations of graphs.

4 RESULTS

4.1 Initial studies on monolayer cell cultures

Monolayer cell cultures provide a simple *in vitro* system for assessment of GC-induced skin atrophy. Normal human dermal fibroblasts and epidermal keratinocytes can be treated by systemical application of GCs and subsequently analysed for atropogenic markers. However, crosstalk between different cell species and particularly between subsets of differentiated cells of one cell species is very limited. Moreover, measuring epidermal thickness and dermal thinning as well as the application of topical formulations are advantages of organotypic 3D culture systems.

4.1.1 mRNA expression

Previous molecular biology studies on monolayer cell cultures performed in the same laboratory (74) confirmed *COL1A1* and *COL3A1* in dermis and *MMP1* in epidermis as predictable read-out parameters for GC-induced skin atrophy. The impact of GCs on *COL4A1* and *COL1A2* expression in fibroblasts was also investigated, however no significant regulation of these gene expression was observed. In addition, a dose-dependent and GC class-specific reduction of IL-6 release into culture supernatants was confirmed by ELISA. In this study, intial studies on monolayer cell cultures were carried out to investigate additional potential read-out parameters for GC-induced skin atrophy prior determining potential atrophy markers on reconstructed skin models.

Keratinocytes and fibroblasts were isolated from foreskin biopsies of young donors provided by local hospitals. Primary human fibroblasts and keratinocytes were stimulated with two different GCs, prednicarbate (PC) and clobetasol 17-propionate (cP). The selected substances represent glucocorticoids with diverse anti-inflammatory potencies (cP class IV > PC class II/III) and different potential to induce skin atrophy (cP > PC), thus allowing an evaluation of their relative effect on collagen synthesis. Two different concentrations, 1 and 100 nM, of GCs were selected. Ethanol and DMSO were used as solvent for PC and cP, respectively. Solvent type and concentration was chosen based on preliminary studies showing no effect on cell proliferation and on collagen and *MMP* gene expression (data not shown). The cells were incubated with test substances and solvents for 72 hours.

Prior determining atrophogenic properties of GCs on reconstructed skin models, collagens of dermal-epidermal junctions *COL7A1* and *COL17A1* as well as extracellular glycosaminoglycan hylauronan synthase (*HAS*)*2* were investigated in cellular assays.

Collagen of dermal-epidermal junction *COL7A1* mRNA was investigated in fibroblasts and keratinocytes with Q-RT-PCR. Interestingly, *COL7A1* mRNA was expressed at higher levels in keratinocytes compared to fibroblasts. In keratinocytes, pre-treated with TNF, a slight downregulation of *COL7A1* mRNA was observed after 72 h stimulation with PC at both concentrations whereas cP slightly upregulated gene expression. In TNF-pretreated fibroblasts, a 2-fold upregulation was detected with Pc and a slight downregulation with cP. In fibroblasts, both GCs slightly increased *COL17A1* expression (data not shown).

Fibroblasts expressed very low levels of *COL17A1*, thus no correlations to GC-treatment were possible. Most interestingly, downregulation of *COL17A1* mRNA was observed in keratinocytes after 72 h of treatment with both GCs. In TNF-pretreated keratinocytes, PC slightly reduced *COL17A1* mRNA while both concentrations of cP induced gene expression by 3-fold (data not shown).

Extracellular matrix hyaluronan synthase (*HAS2*) was investigated in fibroblasts, treated with GCs for 72 h. The lower concentrations of both GCs, PC and cP, reduced *HAS2* expression by 39% and 40%, respectively. In contrast, GCs applied at higher concentrations (100 nM) slightly induced *HAS2* mRNA levels (data not shown).

4.2 Studies on reconstructed skin models

Reconstructed skin models represent a link between *in vitro* monolayer cell cultures and *in vivo* systems with the advantage that fibroblasts and keratinocytes can communicate with each other. Keratinocytes are arranged in multilayer cell structures and thereby, epidermal thickness and dermal thinning can be determined in histological sections as a skin atrophy parameter.

The impact of GCs on reconstructed skin models was assessed by topical application of two GC-containing creams, Dermatop (PC, 0.25%) and Dermoxin (cP, 0.05%). The commercially available GC creams were selected based on their different strength and atrophogenic potential (Dermatop < Dermoxin) and results were compared with Dermatop and DAC base creams, respectively. The amount of applied cream was chosen with respect to the clinically applied dose (10 µl/cm^2). Inflammatory conditions were induced systemically by TNF in one sample. Overall, treated tissue models were compared to untreated control and GC-treated to base cream treated skin models. GC creams, base creams and TNF were applied every second day simultaneously to the media changes, if not mentioned otherwise. Thus, three 14-day treatments were performed in duplicates on MatTek EpidermFT models in all experiments with the exception of one, where effects were evaluated after 14 and 7 days of treatment. Moreover, one experiment with Phenion models was performed for 7 days under the same experimental conditions. All reconstructed skin models were investigated for IL-6 release, collagen and MMP gene expression, epidermal thickness and dermal thinning.

4.2.1 EpidermFT, MatTek

4.2.1.1 Determination of anti-inflammatory effects of GC-containing creams

Prior determining the atrophogenic properties, it was essential to confirm the known anti-inflammatory effects of GCs in the tissue models; therefore cell-free supernatants were collected during the experiments for IL-6 quantification.

As expected, a GC-class-specific reduction of IL-6 release was observed following topical application of GC-containing creams compared to untreated control (Figure 9).

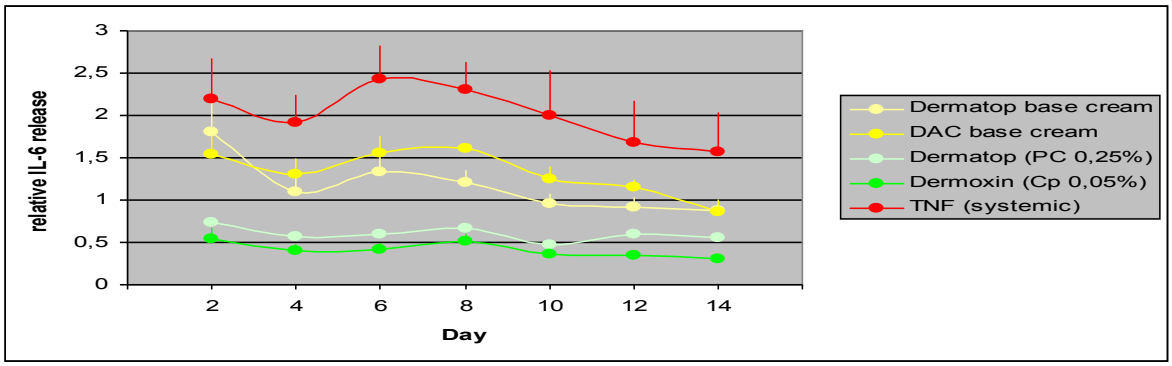

Figure 9: Anti-inflammatory effects of GC treatment of EpidermFT models. The results were determined by measuring IL-6 release with ELISA during 14 days of experiment. Reconstructed skin models were treated every second day with topical GC creams (Pc, 0.25% and cP 0.05%) and topical base creams. TNF was added systemically in one tissue model simultaneously to the medium changes. Each curve represents the mean with standard error mean of three independent experiments performed in duplicates. One duplicate of one experiment lasted 7 days. Medium in one duplicate was changed every day, thus the mean of values from two days following the treatment was calculated for this individual experiment. Values are set relatively to untreated controls (controls are assign as 1.0 in each point of each experiment).

Surprisingly, topical application of base creams alone resulted in an increase of IL-6 release compared to untreated control. It is likely that the mechanical irritation during topical cream application or an ingredient in creams contributed to this induction. Inflammatory conditions were mimicked by systemic TNF treatment, which caused a pronounced IL-6 increase. Interestingly, we observed IL-6 downregulation by repeated doses of TNF. Noteworthy, the anti-inflammatory effects of two different GC creams were monitored for the first time in reconstructed skin models during a longer period of treatment (14 days) and the results confirmed the anti-inflammatory action for repeated application.

4.2.1.2 Regulation of gene expression after treatment with GC-containing creams

After confirmation of the anti-inflammatory effects, the impact of GC-treatment on expression of selected genes was evaluated by Q-RT-PCR. *COL1A1*, *COL3A1*, *COL4A1*, *COL7A1*, *COL17A1*, *MMP1*, *MMP2* and *MMP9* were tested as potential atrophy markers. In addition, IL-6 mRNA expression was measured to compare the anti-inflammatory effects at gene and protein level. To study whether the effects are specific for keratinocytes or fibroblasts, epidermal and dermal compartments of reconstructed skin models were analysed separately.

Surprisingly, only very small amounts of total RNA were detected in the epidermis after 14 days of treatment which correlates with decreased epidermal thickness confirmed by histological analysis. *ALDOA* and *RPLP0* were used as housekeeping genes, since they were identified in the initial studies as the most stable expressed housekeeping genes in the epidermis. As expected, collagens were expressed at very low levels in the epidermis (data not shown). Dermatop (Pc, 0.25%) decreased *MMP1* expression by 2,5-fold compared to Dermatop base cream (Figure 10) (**A**). Similarly, treatment with Dermoxin (Cp, 0.05%) downregulated *MMP1* expression in comparison with DAC base cream. However, different ingredients of Dermoxin and DAC base cream make a direct comparison difficult and hamper the quantitative evaluation of cP-related effects. Increased *MMP1* levels were detected in all samples compared to untreated control.

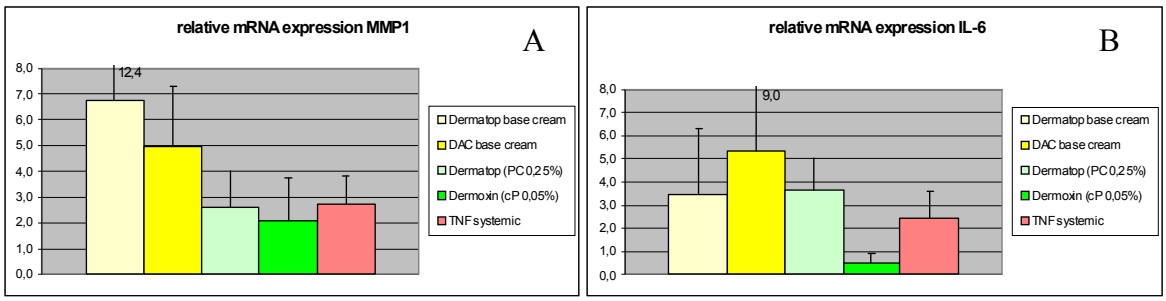

Figure 10: *MMP1* and *IL-6* mRNA expression levels in epidermis of EpidermFT models. Samples were harvested after 14 days of treatment and analysed by Q-RT-PCR. Reconstructed skin models were treated every second day topically with GC creams (Pc, 0.25% and cP 0.05%) and base creams. TNF was added systemically simultaneously to medium changes to one sample. Each bar represents the mean with standard error mean of three independent experiments. Expression values are normalized to *ALDOA* and *RPLP0* and relative to untreated controls (controls are assign as 1.0).

IL-6 mRNA levels in the epidermis were not repressed by Dermatop after 14 days (**B**). Higher levels of *IL-6* appeared in all treated samples with the exception of Dermoxin cream, which supressed cytokine expression by 46% compared to untreated skin models. Of note, histological pictures demonstrated that after the 14-days treatment period the majority of epidermal keratinocytes were found on the margins of the skin models, thus questioning a reliable gene expression analysis of the epidermal compartment.

In contrast, the results for the dermal compartments appear to be more concise (Figure 11).

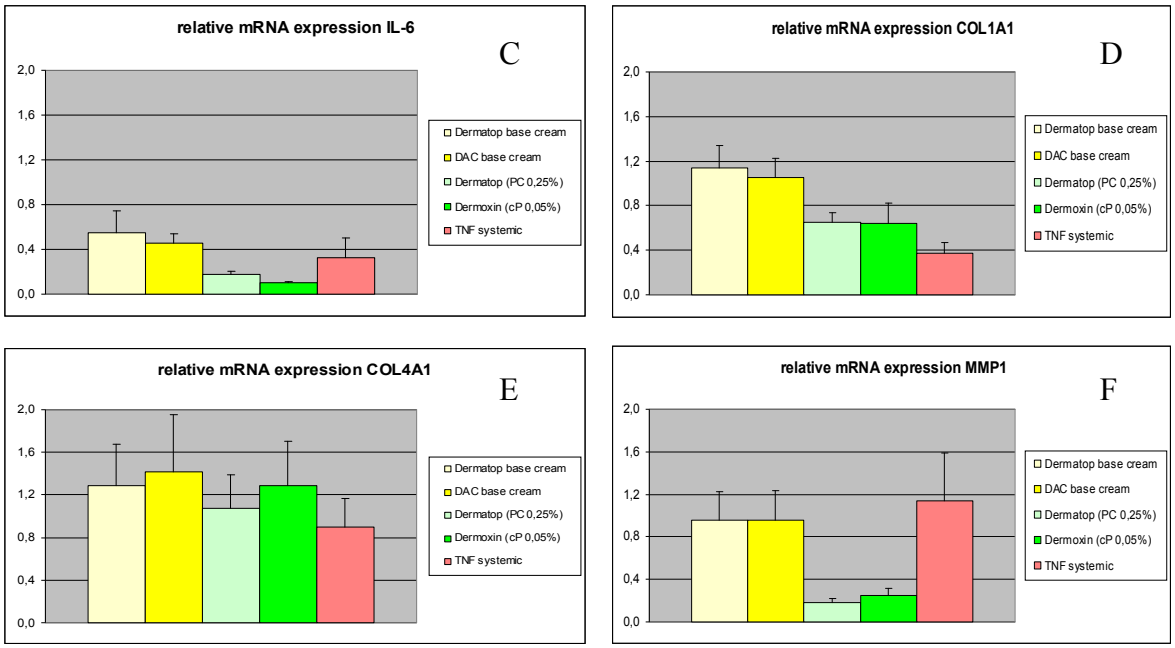

Figure 11: *IL-6*, *COL1A1*, *COL4A1* and *MMP1* mRNA expression levels in dermis of EpidermFT models. The gene expression was measured by Q-RT-PCR after 14 days of treatment. Reconstructed skin models were treated topically every second day with base creams and GC-containing creams (Pc, 0.25% and cP 0.05%), TNF was added systemically simultaneously to medium changes in one sample. Each bar represents the mean with standard error mean of three independent experiments. Expression values are normalized to *ALDOA* and *YWHAZ* and relative to untreated controls (controls are assign as 1.0).

The analyses revealed a GC-class-specific downregulation of *IL-6* and downregulation of *MMP1* and *COL1A1* by both GCs (Graph). The latter **(D)** was downregulated by almost 2-fold when comparing Dermatop (Pc, 0.25%) to Dermatop base cream. Both GCs, Pc and Cp, reduced *COL1A1* mRNA expression, by 35% and 36%, respectively, compared to untreated control. Moreover, *COL1A1* mRNA was reduced by systemic TNF-treatment by 63%. A slight upregulation of *COL1A1* levels was detected with both base cream formulations, which was in agreement with immunofluorescence analysis of collagen I. In

contrast, downregulation of *COL3A1* mRNA appeared only with the more potent GC Cp (data not shown). Decreased levels of *COL3A1* were observed only in TNF and Dermoxin (cP 0.05%), GC of stronger potency, treated samples compared to untreated control. *COL4A1* gene expression was slightly decreased with GC-containing creams compared to complementary base creams **(E)**. *COL17A1* and *COL7A1* were expressed only at very low levels in the epidermal and dermal compartments, thus no quantitative analysis could be performed (data not shown). *MMP1* expression in the dermis was investigated as another potential marker for GC-induced skin atrophy **(F)**. Most interestingly, downregulation of *MMP1* mRNA appeared in dermis 5-fold comparing Dermatop to Dermatop base cream and almost 4-fold comparing Dermoxin to DAC base cream. Noteworthy, base creams values were similar to untreated control, whereas systemic TNF treatment caused a slight increase of *MMP1* expression by 14%. In general, MMPs were expressed at very low levels compared to collagens, with *MMP2* and *MMP9* being hardly detectable in cream-treated samples, while expected levels were determined in controls and systemically TNF-treated samples. High upregulation of *MMP9* mRNA was observed in TNF-treated samples (data not shown). In agreement with analysis of cytokine secretion, GCs inhibited also cytokine expression in a GC-class-specific way. After 14 days, *IL-6* mRNA levels were reduced by 82% and 90% after application of Dermatop (Pc 0,05%) and Dermoxin (cP 0.05%) cream, respectively, compared to untreated control **(C).** Dermatop (Pc, 0.25%) and Dermoxin (cP 0.05%) cream downregulated *IL-6* expression by 3- and 4.5-fold, respectively, when compared to the respective base creams. Overall, results obtained with ELISA at day 14 were well in accordance with Q-RT-PCR

4.2.1.3 Epidermal thickness

In the third part of this study it was tested, whether GC treatment affects epidermal thickness in reconstructed skin models. GC-containing creams were applied topically every second day for 14 days. Histological samples were taken after cessation of the experiment and H&E staining was performed on obtained skin sections (Figure 12).

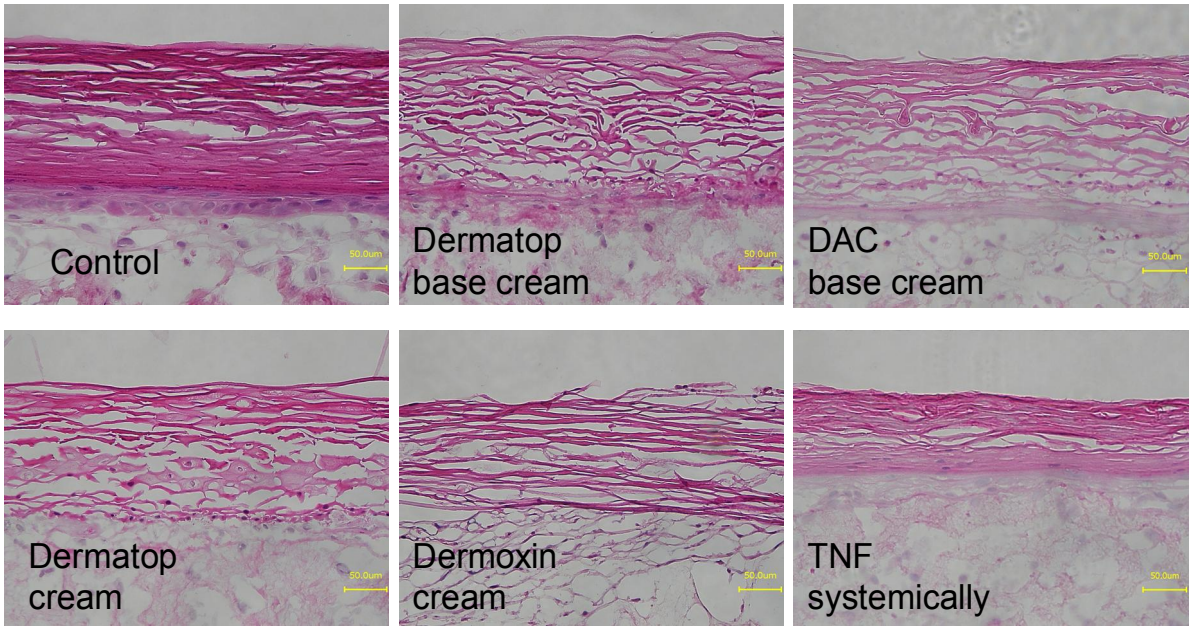

Figure 12: Histological analysis of EpidermFT models. GC-containing creams and base creams were added topically and TNF systemically every other day simultaneously to the media changes for 14 days. The number of keratinocyte layer was determined on 5 µm thick histological sections H&E stained (see Materials and methods.2.2.4) and observed with a digital microscope. Scale bar indicates 50 µm. Exposure time 1/20s. Data are representative of three independent experiments.

After 14 days of incubation untreated control tissues already showed a strongly reduced epidermal thickness. Furthermore, strongly reduced epidermal thickness and injured epidermis was detected after topical application of base creams and GC creams. Thus, measurement of epidermal layers and evaluation of epidermal thickness was not possible. Noteworthy, severe parakeratosis was observed in the epidermis with cell nuclei appearing in the stratum corneum of TNF- and cream-treated tissue models.